Electronic Supporting Information

Self-assembled decanuclear $Na^{I}_{2}Mn^{II}_{4}Mn^{III}_{4}$ complexes: From discrete clusters to 1- and 2-D structures, with the $Mn^{II}_{4}Mn^{III}_{4}$ unit displaying a large spin ground state and SMM behaviour.

Stuart. K. Langley, Nicholas Chilton, Boujemaa Moubaraki and Keith S. Murray

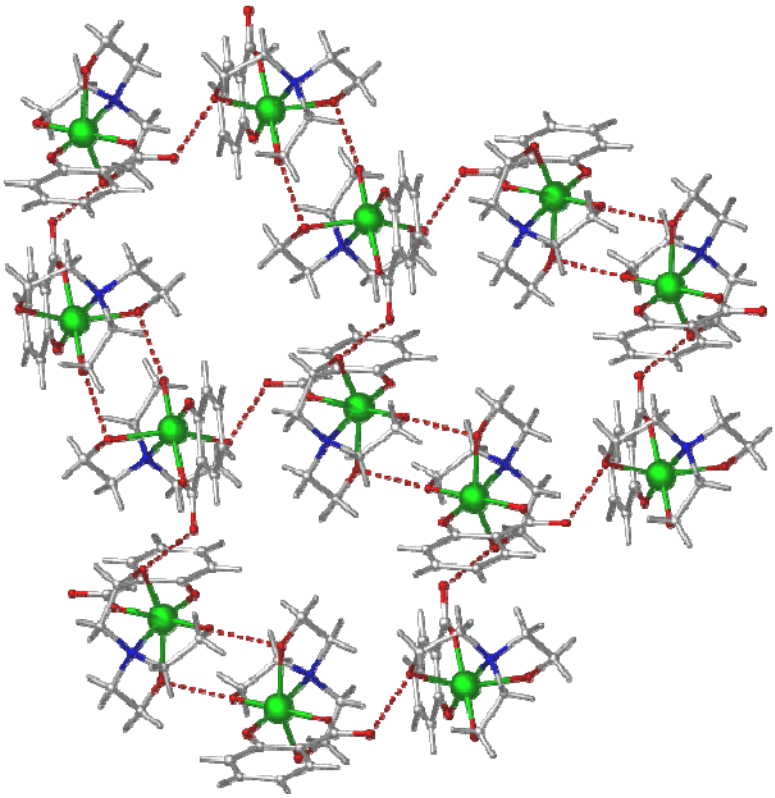

Fig. S1. View of the H-bonded 2-D sheet of **1**.

	(II)	(III)	(IV)
Mn1	3.41	**3.16**	3.11
Mn2	**2.05**	1.92	1.86
Mn3	**1.90**	1.72	1.73
Mn4	3.41	**3.18**	3.13

Table S1. Bond valence sum calculations for **2**. The bold value is the one closest to the charge for which it is calculated.

Mn5-O29	1.877(7)	Mn6-O24	2.266(7)	Mn7-N10^{I}	2.336(9)	K2-O18	2.758(8)
Mn5-O28	1.920(7)	Mn6-O23	2.333(7)	Mn8-O25	1.881(7)	K2-O19	2.932(3)
Mn5-O20	1.936(7)	Mn6-N8	2.428(9)	Mn8-O21	1.909(7)	K2-O27	2.951(8)
Mn5-O30	1.943(8)	Mn6-N10	2.481(9)	Mn8-O18	1.925(8)	K2-O31	3.089(9)
Mn5-O24	2.179(7)	Mn7-O24	2.148(7)	Mn8-O27	1.937(7)	K2-O20	3.185(9)
Mn5-N9	2.362(10)	Mn7-O22^{I}	2.161(7)	Mn8-O22	2.201(8)	K2-O17	3.428(9)
Mn6-O28	2.139(7)	Mn7-O20	2.170(7)	Mn8-N7	2.339(11)		
Mn6-O25^{I}	2.219(6)	Mn7-O27	2.187(8)	K2-O30	2.654(7)		
Mn6-O22	2.258(7)	Mn7-N10	2.300(11)	K2-O31^{II}	2.744(9)		

Table S2. Selected bond lengths for **5.** Symmetry transformations : (I) 2 - x, - y, - z. (II) 1 - x, - y, - z.

	1	**2**	**3**	**4**	**5**
Formula[a]	$MnC_{13}H_{19}O_{6.5}N$	$Na_2Mn_8C_{74}H_{134}O_{40}N_{12}$	$Na_2Mn_8C_{73}H_{130}O_{39}N_{12}$	$Na_2Mn_8C_{72}H_{120}N_{12}O_{35}$	$K_2Mn_8C_{69}H_{118}O_{37}N_{12}$
M_r gmol^{-1}	348.22	2317.43	2285.33	2199.28	2225.54
Crystal system	Monoclinic	Monoclinic	Triclinic	Monoclinic	Triclinic
Space group	*P2$_1$/n*	*P2$_1$/n*	*P-1*	*C2/c*	*P-1*
a/Å	10.0895(2)	17.813(4)	12.8576(3)	25.8728(6)	14.798(3)
b/Å	9.4777(2)	12.949(3)	14.5491(3)	24.3303(5)	18.608(4)
c/Å	15.1121(5)	23.397(5)	14.8713(3)	16.0384(4)	18.879(4)
α/deg	90	90	76.2500(10)	90	77.060(3)
β/deg	93.4790(10)	100.75(3)	68.6450(10)	100.2860(10)	75.811(5)
γ/deg	90	90	84.7590(10)	90	82.295(5)
V/Å^3	1442.44(5)	5302.0(18)	2516.64(9)	9933.8(4)	4894.3(17)
T/K	123(2)	100(2)	123(2)	123(2)	123(2)
Z	4	2	1	4	2
ρ_{calc} [g cm^{-3}]	1.599	1.452	1.503	1.469	1.507
λ[b]/ Å	0.71073	0.71123	0.71073	0.71073	0.71073
Data Measured	16624	34274	28474	35026	22307
Ind. reflns	4439	9284	11452	10121	13515
R_{int}	0.0254	0.045	0.030	0.049	0.050
Reflns with I I > 2σ(I)	4167	8108	9379	8059	8765
Parameters	207	614	552	644	1072
Restraints	6	4	0	75	62
*R*1[c] (obs), *wR*2[c] (all)	0.039, 0.089	0.060, 0.157	0.046, 0.146	0.066, 0.165	0.088, 0.25
goodness of fit	1.050	1.089	1.058	1.068	1.033
Largest residuals/ e Å^{-3}	0.94, -0.50	0.76, -0.83	1.58, -0.52	0.66, -0.76	2.22, -0.96

[a] Including solvate molecules. [b] Graphite monochromator.

[c] $R1 = \Sigma||F_o| - |F_c||/\Sigma|F_o|$, $wR2 = \{\Sigma[w(F_o^2-F_c^2)^2]/\Sigma[w(F_o^2)^2]\}^{1/2}$.

Table S3 Crystallographic data for **1** – **5** with the refinements for **2** – **5** having used program PLATON/SQUEEZE.[see CIFs labelled **2**Na2Mn8 final+sq.CIF, etc]. In each case, all lattice solvent was removed except for one well defined MeOH in **2** and then the SQUEEZE program was run and subsequently re-refined with the final SQUEEZED data set. In all cases, the original chemical formula, including lattice solvent, was retained for consistency with calc. density and F(000).

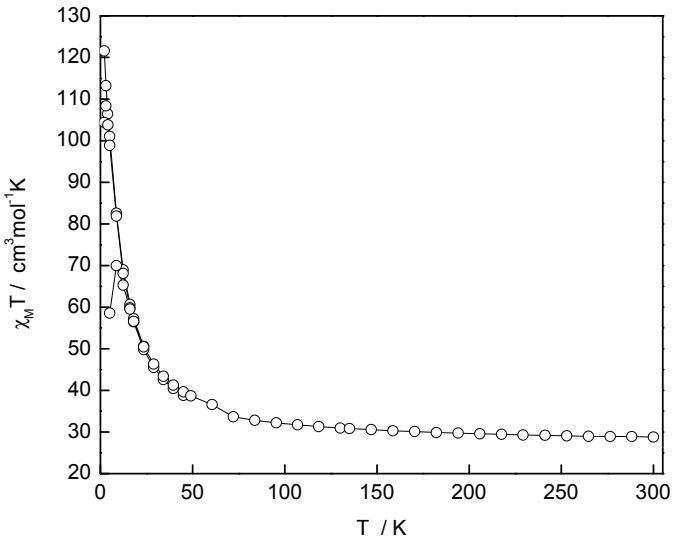

Fig. S2. $\chi_M T$ versus T plot for **2** in DC fields of 1 T (2 – 300 K), 0.1 T and 0.01 T (2 – 70 K).

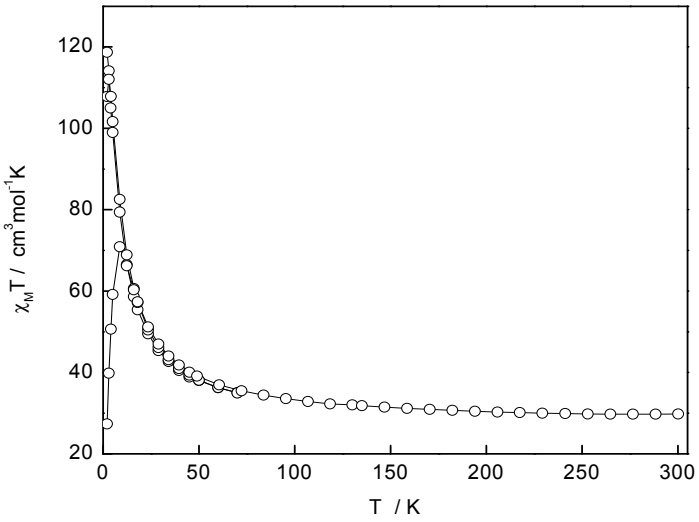

Fig. S3. $\chi_M T$ versus T plot for **4** in DC fields of 1 T (2 – 300 K), 0.1 T and 0.01 T (2 – 70 K).

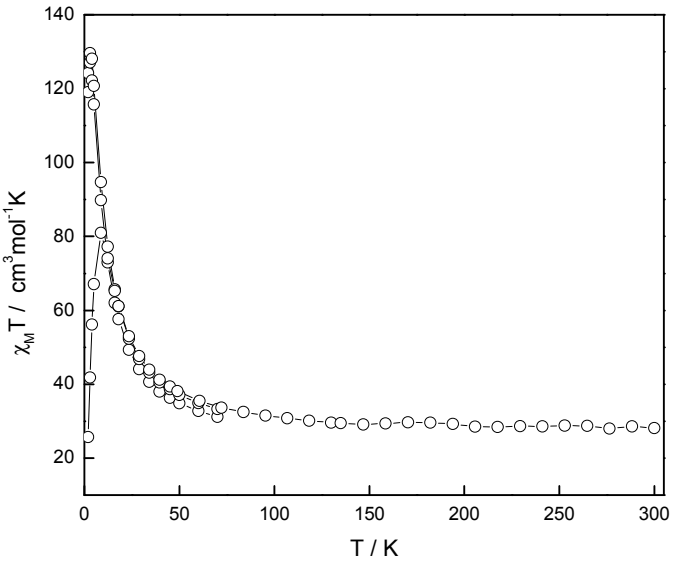

Fig. S4. $\chi_M T$ versus T plot for **5** in DC fields of 1 T (2 – 300 K), 0.1 T and 0.01 T (2 – 70 K).

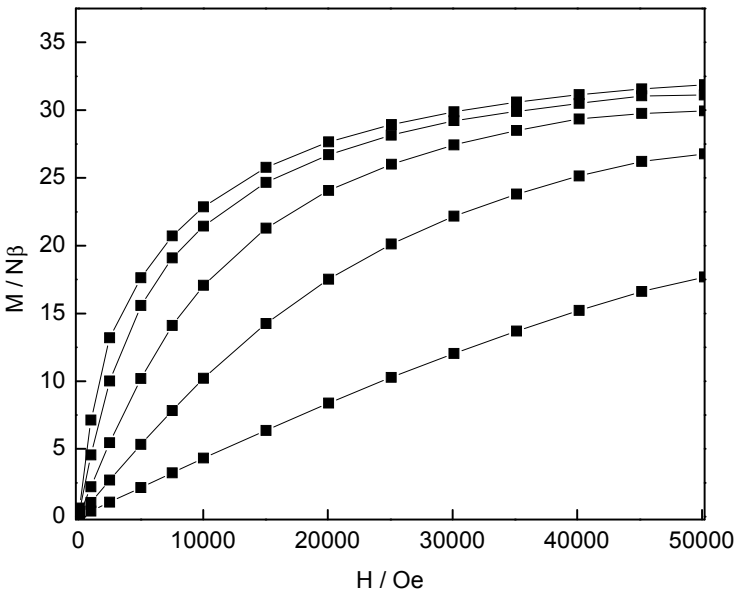

Fig S5. *M* vs *H* isothermal plots for **2** in the 2 (top) – 20 K (bottom) temperature range. The solid lines are guides for the eye.

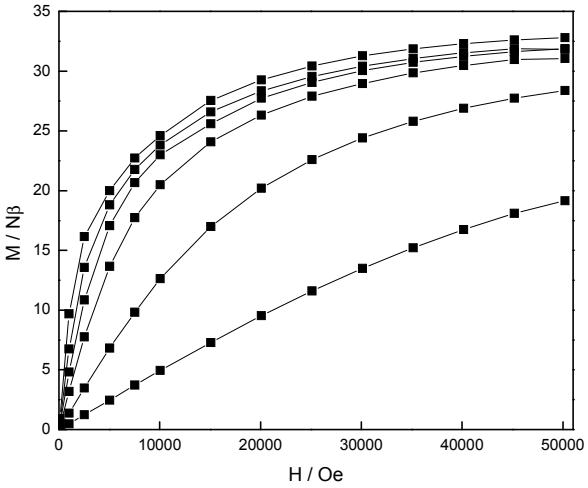

Fig S6. *M* vs *H* isothermal plots for **4** in the 2 (top) – 20 K (bottom) temperature range. The solid lines are guides for the eye.

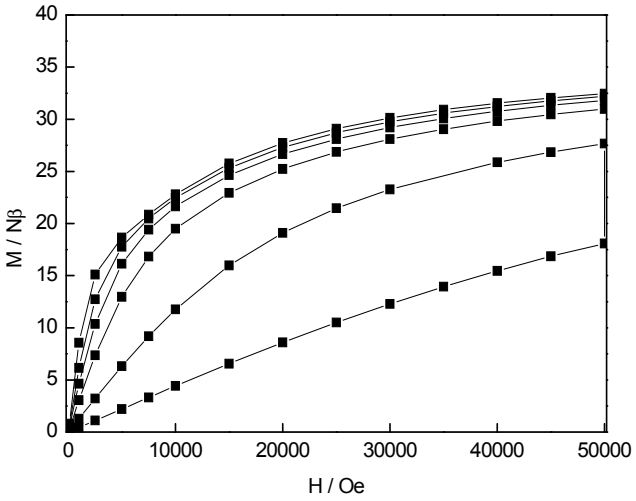

Fig S7. *M* vs *H* isothermal plots for **5** in the 2 (top) – 20 K (bottom) temperature range. The solid lines are guides for the eye.

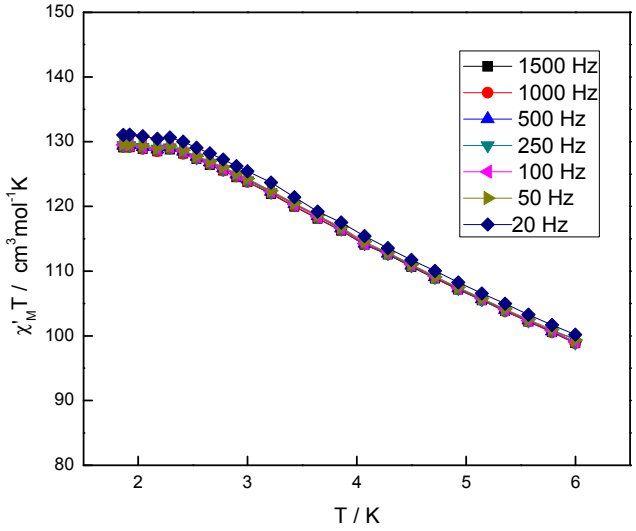

Fig S8. $\chi_M{}'T$ vs. T for **2**.

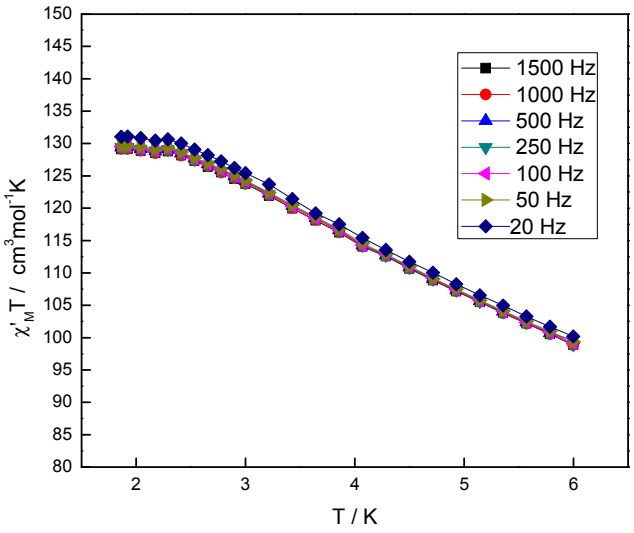

Fig. S9. $\chi_M{}'T$ vs. T for **4**.

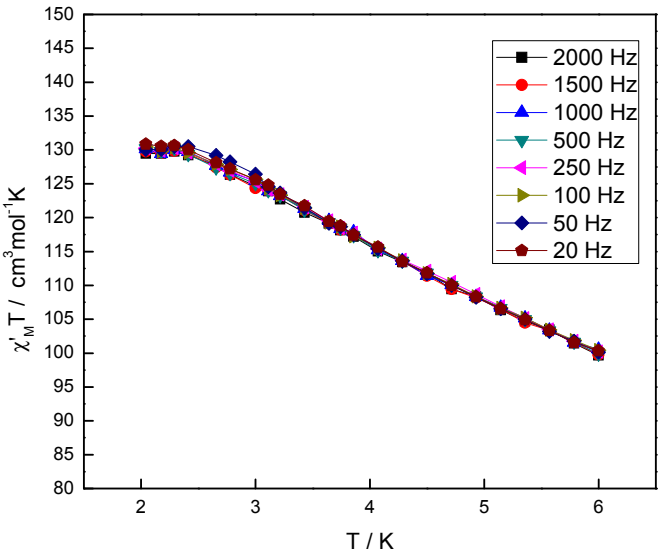

Fig. S10. $\chi_M^{'}T$ vs. T for **5**.

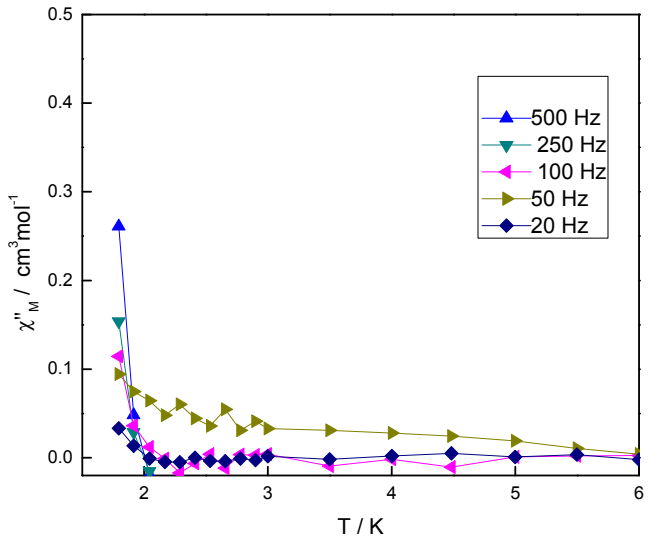

Fig. S11. $\chi_M^{''}$ vs. T for **2**.

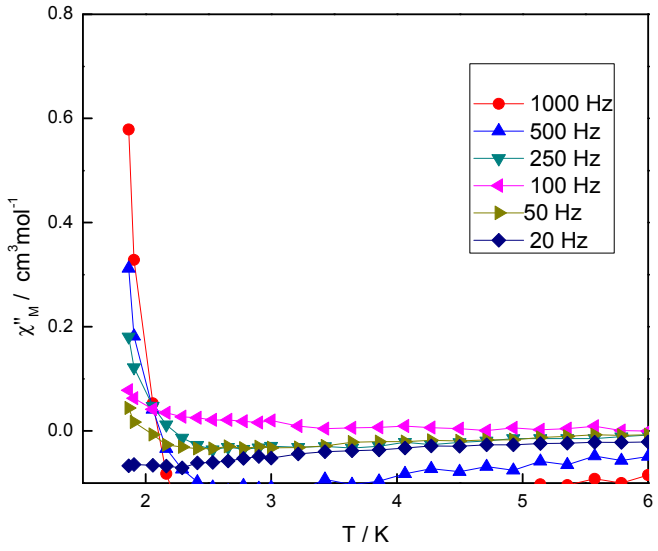

Fig. S12. $\chi_M^{''}$ vs. T for **4**.

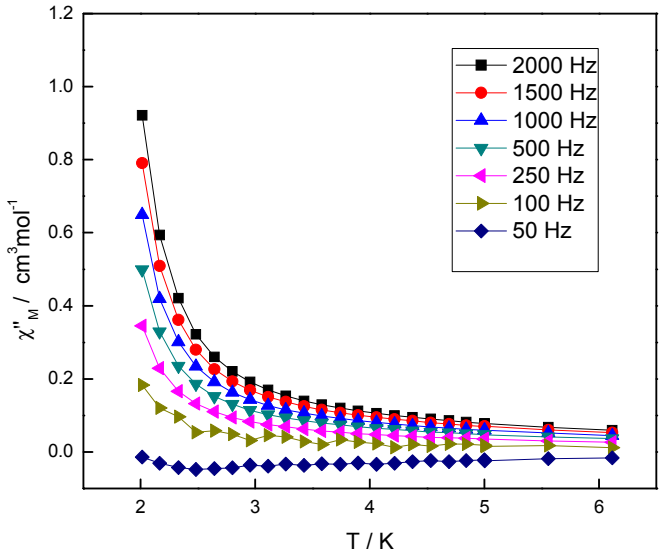

Fig. S13. $\chi_M^{''}$ vs. T for **5**.